Effects of N-ion-implantation and post-thermal annealing on ZnO:Mg thin films

S. W. Xue*, L. X. Shao, J. Zhang
Department of Physics, Zhanjiang Normal College, Zhanjiang 524048, P. R. China

N-ion-implantation to a fluence of 1×10^{17} N^+/cm^2 was performed on ZnO:Mg thin films deposited on fused silica glass substrates by a sol-gel technique. The N-implanted films were annealed in flowing nitrogen at 500-900 ^oC. Damage recovery was investigated by X-ray diffraction (XRD), photoluminescence (PL) and optical absorption measurements. Results showed that diffraction peaks and PL intensities were decreased by N ion implantation, but they partially recovered after thermal annealing. In this experiment, all films exhibited high resistivity and p-type conduction was not observed after N ion implantation.

Keywords: ZnO:Mg films; ion implantation; XRD, Absorbance; Photoluminescence

(Received February 1, 2009; accepted March 22, 2009)

1. Introduction

Zinc oxide (ZnO), a wide band gap semiconductor, has gained substantial interest in the research community due to its potential applications in optoelectronic devices in the blue and ultraviolet region. The main obstacle to the development of ZnO has been the lack of reproducible and low-resistivity p-type ZnO. In recent years, many techniques have been employed to synthesize high-quality ZnO films, such as radio frequency (RF) magnetron sputtering, chemical vapor deposition, pulsed laser deposition, plasma-assisted molecular beam epitaxy (MBE), and the sol-gel process [1-5].

Ion implantation is a widespread tool for doping in the semiconductor industry. It can be used to fabricate doped ZnO films. Advantages of ion implantation are the lateral selectivity of sample area and doping depth as well as an accurate fluence control. Recent theoretical and experimental studies show that nitrogen is a very promising p-type dopant, but its solubility in ZnO is low. Ion implantation and donor-acceptor codoping method are two effective approaches to enhance the solubility limit of nitrogen in ZnO. Several groups have obtained good p-type conduction in ZnO by nitrogen ion implantation. Li et al. suggest that adding small amounts of Mg under appropriate growth conditions can effectively enhance the p-type dopability of ZnO [6], but experiments based on this approach have not been performed yet.

In this work, we report N ion implantation into ZnO:Mg films by the sol-gel process. The

influences of N ion implantation and post-thermal annealing on ZnO:Mg films are investigated.

2. Experimental

2.1 Preparation of ZnO:Mg films and N-ion-implantation

ZnO:Mg thin films used in this study were deposited on fused silica glass substrates by the sol–gel method. Zinc acetate dehydrate ($Zn(CH_3COO)_2 \cdot H_2O$) was used as a starting material. Monoethanolamine (MEA) and 2-methoxyethanol were used as stabilizer and solvent, respectively. The Mg dopant source is $Mg(CH_3COO)_2 \cdot 4H_2O$. For Mg doping, zinc acetate dihydrate and $Mg(CH_3COO)_2 \cdot 4H_2O$ were first dissolved in a mixture of 2-methoxyethanol and MEA solution at room temperature. The atomic ratio of Mg/Zn is 0.25:0.75. The molar ratio of MEA to zinc acetate ($Zn(CH_3COO)_2$) was maintained at 1.0 and the concentration of zinc acetate was 0.35 M. The solution was stirred at 60 ^oC for 2 h to yield a clear and homogeneous solution, which served as the coating solution after cooling to room temperature. The coating was usually made 24 hours after the solution was prepared. The solution was dropped onto fused silica glass substrates, which were rotated at 4000 rpm for 30 s. After depositing by spin coating, the films were dried at 300 ^oC for 10 min over a hot plate to evaporate the solvent and remove organic residuals. In this experiment, to eliminate the influences of un-implanted layer on the structural, optical and electrical properties of ZnO:Mg we repeated the procedures from coating to drying only three times. The films were then put into a quartz tube furnace and annealed in air at 500 ^oC for 1h. The average thickness of the films chosen was about 250 nm measured by an OLYMPUS BX51 interference/transmission microscopy.

The as-prepared ZnO:Mg films were subjected to N ion implantation at 56 keV to a fluence of 1×10^{17} N^+/cm^2. Fig.1 showed the depth profile of implanted N atoms simulated using the code TRIM 96.

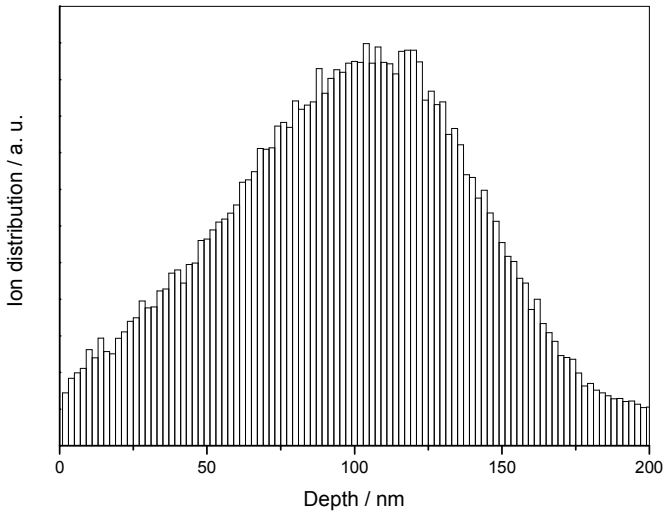

Figure 1 TRIM simulation of the depth profile of implanted N atoms for ZnO:Mg films.

The projected range (R_p) of the atoms was about 96 nm. The maximum depth of implanted N ions is roughly equal to the thickness of ZnO:Mg films. After ion implantation, N-implanted films were annealed in flowing nitrogen at 500-900 ^oC for 1h in a quartz tube furnace.

2.2 Measurements

To characterize the structural and optical properties of the as-prepared and N-implanted films, the crystal orientation was investigated using a PHILIPS X'PERT PRO MPD X-ray diffractometer (XRD) with the radiation source of CuKα. Optical absorbance was measured using a SHIMADZU UV2550 spectrophotometer. Room temperature (RT) photoluminescence spectra (PL) were recorded by a SHIMADZU RF5301PC spectrophotometer with excitation wavelength of 345 nm. The resistivity of the films was measured by the four-point probe method.

3. Results and discussion

3.1 Structural properties

To investigate the effects of annealing on the structural properties of N-implanted ZnO:Mg films, the films were annealed in flowing nitrogen at different temperatures from 500 to 900 ^oC for 1h after N ion implantation. Fig.2 shows XRD patterns of ZnO:Mg films after N ion implantation and annealing at different temperatures. For comparison, we also add XRD patterns of ZnO:Mg films before and after N ion implantation.

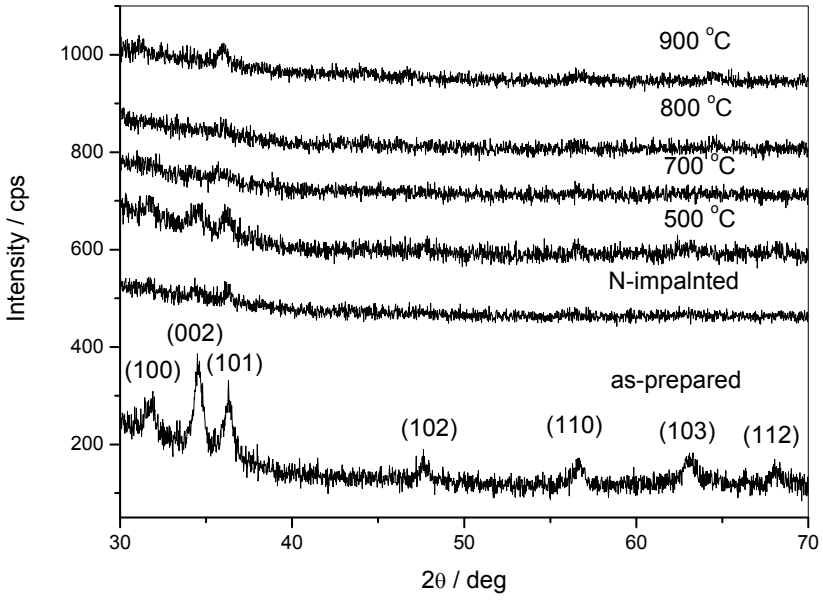

Figure 2. XRD patterns of ZnO:Mg films after N-implantation and post-thermal annealing at different temperatures.

It can be seen that all films still show the hexagonal wurtzite structure after N ion

implantation and post-thermal annealing. No evidences of any other secondary phases and impurities are found in the XRD patterns. Though ZnO is a radiation-hard material, we can see that the intensities of all diffraction peaks were greatly decreased by N ion implantation. The decreases of diffraction peaks can be attributed to ion-beam induced lattice disorder. Thermal annealing has evident influences on the structural properties of N-implanted films. Fig.2 shows that diffraction peaks partially recover after annealing at 500 ^{o}C for 1 h. The enhancement of diffraction peaks are due to the annealing-out of ion-beam induced defects. However, the intensities of all peaks decrease with increasing annealing temperature when it exceeds 500 ^{o}C. Similar results are also found in Zn-implanted ZnO films [7] and N-implanted ZnO:Al films (to be published). We ascribe the decreases of all peaks with increasing annealing temperatures mainly to the thermal induced lattice disorder at high temperature. Though we have observed the recoveries of all diffraction peaks in Zn-implanted ZnO films and N-implanted ZnO:Al films, it is noted that the recovery does not occur in N-implanted ZnO:Mg films. We will further discuss this difference in the following section.

3.2 Optical properties

Fig.3 shows the influences of N ion implantation and post-thermal annealing on the optical absorption of N implanted ZnO:Mg films. It can be seen from Fig.3 that the optical absorption was enhanced distinctly in the visible region after N ion implantation.

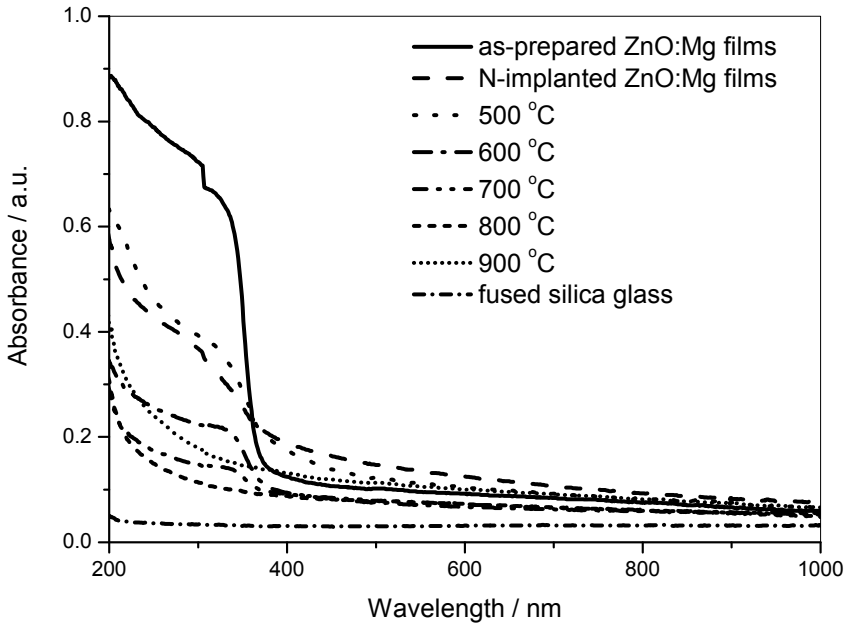

Figure 3 Optical absorption spectra of ZnO:Mg films after N-implantation and post-thermal annealing at different temperatures.

Subsequent annealing has evident influence on the optical absorption of N-implanted ZnO:Mg films. It is found that the optical absorption in the visible region decreases with increasing annealing temperatures from 500 - 800 ^{o}C while increase when annealing

temperature exceeds 800 °C. We have also observed similar results in Zn-implanted ZnO films and N-implanted ZnO:Al films. We ascribe the decrease and increase of optical absorption mainly to the annealing out of ion-beam induced defects and the thermal induced defects at high temperatures, respectively [7]. What makes it different in this experiment is the disappearance of absorption edge at high temperatures of 800 – 900 °C. We can clearly see the disappearance of absorption edge in Fig.3 when annealing temperature exceeds 800 °C. Dart has found that the evaporation rate of ZnO increases rapidly with temperature when it exceeds 600 °C [8]. Coleman et al. found that the heavily damaged As-implanted ZnO layer is almost completely decomposed and evaporated at 1200 °C [9]. Therefore, we temporarily ascribe this abnormal phenomena to the decomposition and evaporation of N-implanted ZnO:Mg films at high temperatures though much work needs to be done to confirm this. In this experiment, the thickness of ZnO:Mg films is roughly equal to the maximum depth of implanted N ions. So, the influences of un-implanted layer on the structural and optical properties can be neglected. In other experiments [7], we did not observe the disappearance of absorption edge at high annealing temperatures due to the existence of thick um-implanted ZnO layer. We think that the thickness of ZnO:Mg films becomes very thin after annealing at 800 - 900 °C due to the rapid decomposition and evaporation. Fig.3 also shows a comparison of the absorbance spectra of N-implanted ZnO:Mg with that of fused silica glass substrate. Though the shapes of the spectra of N-implanted ZnO:Mg films after annealing at 800 – 900 °C are similar to that of the substrate, it can be seen that the absorbance is still larger than that of the substrate, indicating the residual existence of the N-implanted ZnO:Mg films. Due to the heavy reduction of the thickness of the N-implanted ZnO:Mg films, the characteristic absorption of ZnO:Mg can not be clearly detected by the spectrophotometer. We think that this may be the main reason why diffraction peaks only partially recover during the post-thermal annealing from 500-900 °C.

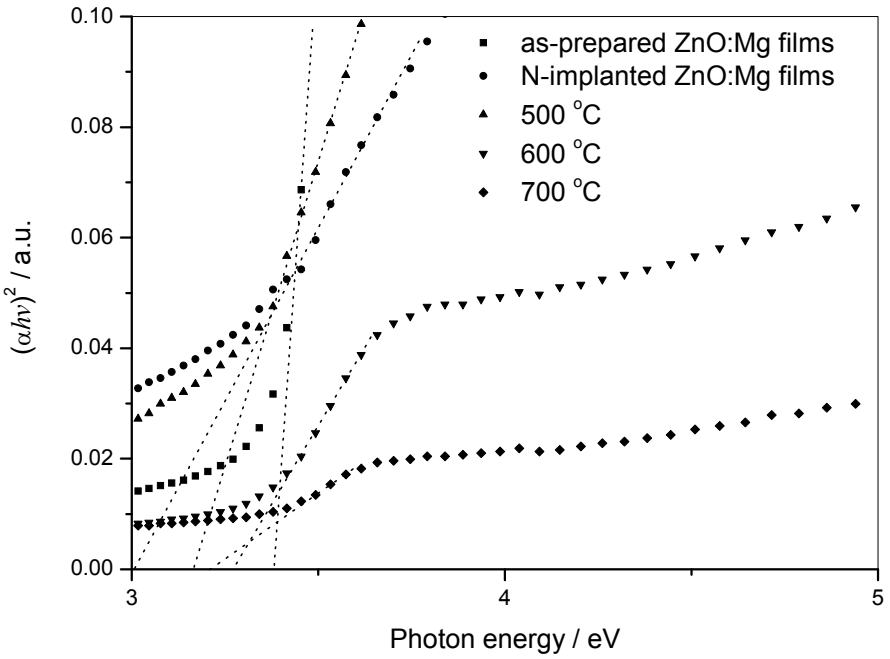

Figure 4 $(\alpha hv)^2 \sim hv$ plots of ZnO:Mg films before and after N-implantation.

In addition, N ion implantation and post-thermal annealing also have evident influences on the optical bandgaps of ZnO:Mg films as shown in Fig.4 and Table 1.

Table 1 Optical bandgaps of ZnO:Mg films before and after N ion implantation.

Annealing temperature / °C	As-prepared	N-implanted	500	600	700	800	900
Optical bandgap / eV	3.38	3.02	3.16	3.27	3.21	?	?

The optical bandgaps are determined from the conventional method [10]. As the absorption edge disappears after annealing at 800 - 900 °C, we do not know the bandgaps of N-implanted ZnO:Mg films at these stages. It can be seen that the optical bandgap redshifts after N ion implantation. Subsequent annealing between 500 and 600 °C makes the optical bandgap blueshift while redshift when annealing temperature exceeds 600 °C. Similar results are also found in Zn-implanted ZnO films. We attribute the observed behaviors of the optical bandgaps mainly to the changes of defect concentrations in ZnO films. It is believed that many defects are produced during Zn ion implantation. They may cause the redshift of the optical bandgap. Most of the ion-beam induced defects are annealed out by the subsequent annealing from 500 to 600 °C. This results in the buleshift of bandgap due to the decrease of defect concentration in ZnO:Mg films. During the following annealing stage between 600 and 900 °C, thermal induced defects at high temperatures increase dramatically, which leads to the redshift of the optical band edge again due to the increase of defect concentration with annealing temperatures.

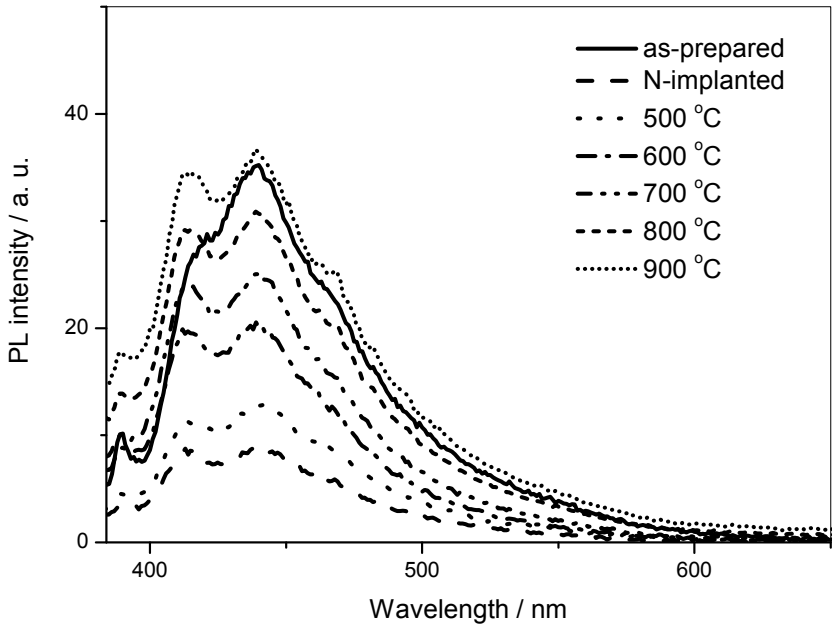

Figure 5 RT PL spectra of ZnO:Mg films after N-implantation and post-thermal annealing at different temperatures (Excitation wavelength: 345nm).

Fig.5 shows RT PL spectra of ZnO:Mg films after ion implantation and annealing at different temperatures from 500 to 900 ^{o}C. The shape of all the spectra, similar to those reported by others [11-13], is featured by a near band edge (NBE) excitonic UV emission and a defect related deep level emission (DLE) in the visible region. It can be seen that NBE and DLE are decreased after N ion implantation. The decreases are mainly due to the ion-beam induce defects which serves as non-radiative centers [14]. Compared with Ref.14, it is noted that PL emission is not completely extinguished in our experiment. We have observed similar results in Zn-implanted ZnO films and N-implanted ZnO:Al films. We think that this difference may be due to different implantation conditions and properties of the material used in the experiments (single crystal ZnO was used in Ref.14). Subsequent annealing has pronounced influences on the emission properties. Both NBE and DLE increase with increasing annealing temperatures from 500 to 900 ^{o}C.

3.3 Electrical properties

Li et al. shows that the acceptor transition energy of N_O-nZn_{Zn} can be reduced if we replace Zn by isovalent Mg to reduce the anion and cation kinetic *p-d* repulsion, as well as the electronic potential, because unlike Zn, Mg has no occupied *d* orbitals [6]. However, type conversion in N-implanted ZnO:Mg films was not observed in this experiment. The resistivity of ZnO:Mg and N-implanted ZnO:Mg films was measured with the four-point probe method at every processing stage. We found that they all exceeded the measurement range of 10^5 cm·Ω. All films exhibited high resistivity at any stages. In case of high resistivity, we can not identify the conduction type of N-implanted ZnO:Mg films by Hall effect measurements. As all films in our experiment exhibit high resistivity, we think that isovalent Mg does not effectively replace Zn as expected. Shan found that as more Mg was introduced into ZnO film, Mg lodges itself in an interstitial position [15].

4. Conclusions

ZnO:Mg films are prepared on fused silica glass substrates by sol-gel method. N ion implantation to a fluence of 1×10^{17} N^+/cm^2 has caused structural and optical changes to ZnO:Mg films. After N-implantation of ZnO:Mg films, all films still remains single phase and hexagonal wurtzite structure. XRD intensities and PL emissions are greatly decreased by N ion implantation. Post-thermal annealing does not cause the full recoveries of the structural and optical properties of N-implanted ZnO films. With increasing annealing temperature, both NBE and DLE increase. all films exhibit high resistivity and P-type conduction is not observed after N ion implantation and post-thermal annealing.

Acknowledgements

S W Xue is grateful to Dr. Jingbo Li, first author of Ref.6, for helpful discussions on the

Mg doping concentration. This work was supported the Special Foundation for University Subject Construction of Department of Education of Guangdong Province under Project No. [2006] 11.

References

[1] T. L. Yang, D. H. Zhang, J. Ma, H. L. Ma, Y. Chen, Thin Solid Films **326** (1998) 60.
[2] Y. Zhou, P. J. Kelly, A. Postill, O. Abu-Zeid, A. A. Alnajjar, Thin Solid Films **447-448** (2004) 33.
[3] T. M. Barnes, J. Leaf, C. Fry, C. A. Wolden, J. Crystal Growth 274 (2005) 412.
[4] J. Mass, P. Bhattacharya, R. S. Katiyar, Mater. Sci. Eng. **B. 103** (2003) 9.
[5] V. Musat, B. Teixeira, E. Fortunato, R. C. C. Monteiro and P. Vilarinho, Surf. Coat. Tech. **180-181** (2004) 659.
[6] J. B. Li, S. H. Wei, S. S. Li, J. B. Xia, Physical Review B. **74** (2006) 081201.
[7] S.W. Xue, X.T. Zu, L.X. Shao, Z. L. Yuan, W. G. Zheng, X. D. Jiang, H. Deng, Journal of Alloys and Compounds. doi:10.1016/j.jallcom.2007.04.239.
[8] F. E. Dart, Physical Review **78** (1950) 761.
[9] V. A. Coleman, H. H. Tan, C. Jagadish, S. O. Kucheyev, J. Zou, Appl. Phys. Lett. **87** (2005) 231912.
[10] N. Kenny, C. R. Kannewurf, D. H. Whitmore, J. Phys. Chem. Solids **27** (1966) 1237.
[11] S. Fujihara, Y. Ogawa, A. Kasai, Chem. Mater., 16 (2004) 2965.
[12] X. D. Gao, X. M. Li, W. D. Yu, Materials Research Bulletin **40** (2005) 1104.
[13] R. J. Hong, J. D. Shao, H. B. He, Z. X. Fan, Journal of Crystal Growth 290 (2006) 334.
[14] I. Sakaguchi, D. Park, Y. Takata, S. Hishita, N. Ohashi, H. Haneda, T. Mitsuhashi, Nuclear Instruments and Methods in Physics Research **B 206** (2003) 153.
[15] F. K. Shan, B. I. Kim, G. X. Liu, Z. F. Liu, J. Y. Sohn, W. J. Lee, B. C. Shin, Y. S. Yu, J. Appl. Phys. **95** (2004) 4772.

*Corresponding author: xueshuwen@263.net